Phenotypic characterization of *Lith* genes that determine susceptibility to cholesterol cholelithiasis in inbred mice: physical-chemistry of gallbladder bile[1]

David Q-H. Wang, Beverly Paigen,* and Martin C. Carey[2]

Department of Medicine, Harvard Medical School, Gastroenterology Division, Brigham and Women's Hospital, and Harvard Digestive Diseases Center, Boston, MA 02115, and The Jackson Laboratory,* Bar Harbor, ME 04609

Abstract *Lith* genes control susceptibility to cholesterol gallstone formation in inbred strains of mice on a lithogenic diet containing high fat, high cholesterol and 0.5% cholic acid. Our study defines the physical–chemical phenotypes of C57L, AKR, and (C57L × AKR) F_1 mouse gallbladder biles during 56 days on the lithogenic diet. We found enhanced cholesterol supersaturation, accumulation of mucin gel, and larger gallbladders in all C57L and F_1 mice, as well as more frequent gallstone formation in male C57L and F_1 mice (80%) compared to females (40%) or AKR mice (15%). In male C57L and F_1 mice, mucin gel accumulated at 3 days, followed by cholesterol supersaturation and phase separation of liquid crystals, solid monohydrate crystals, and, in 43% of mice, anhydrous cholesterol crystals; whereas, in females, phase separations were delayed 2 to 9 days, and anhydrous crystals did not form. In AKR mice, cholesterol supersaturation and phase separations were infrequent and delayed, and gender did not influence the phenotype. Taurocholate invariably replaced endogenous bile salts, especially tauro-β-muricholate, with crystallization sequences matching taurocholate-containing model bile systems. We conclude: *i*) *Lith* genes determine biliary cholesterol supersaturation, mucin gel accumulation, gallbladder size, phase-separation, and prevalence of cholesterol gallstones. *ii*) Identical phenotypes in C57L and F_1 mice indicate susceptibility to cholesterol gallstones is genetically dominant, favoring males 2:1. *iii*) Mucin gel accumulation, crystallization, and stone formation are rare in AKR mice. This definition of the physical chemistry of lithogenesis should aid in further elucidation of the *Lith* genes and the proteins they encode.—**Wang, D. Q-H., B. Paigen, and M. C. Carey.** Phenotypic characterization of *Lith* genes that determine susceptibility to cholesterol cholelithiasis in inbred mice: physical-chemistry of gallbladder bile. *J. Lipid Res.* 1997. **38:** 1395–1411.

Supplementary key words gallstones • mucin gel • genetics • anhydrous and monohydrate crystals • microscopy • dominant trait • liquid crystals • phase separation • crystallization • gallbladder size

Cholesterol (Ch) gallstone disease is a major public health problem in all developed countries (1, 2). A genetic predisposition is clearly present in the Pima (3), certain other North American Indians (4, 5), and Chileans (6), populations with very high prevalence and early onset rates (4, 7, 8). Not so well known is that Ch gallstone disease is appreciably more common among family members in Caucasians (9–12). Van der Linden (11) and Huddy (13) reported that gallstones were more frequent by a ratio of 3:1 in siblings and other family members than in spouses or unrelated controls. Using ultrasonography to ascertain gallstones in first-degree relatives of index patients, Gilat et al. (14) found a 21% prevalence in first-degree relatives compared with 9% in matched controls, and Sarin et al. (15) found a 5 times higher frequency than in controls. With respect to bile composition, Danzinger et al. (16) noted that cholesterol supersaturation was higher in fasting duodenal bile of older sisters of Ch gallstone patients than in controls. Pairwise correlations for Ch synthesis, bile saturation, and gallstone prevalence were also significantly higher in monozygotic than in dizygotic male twins (17), underscoring the importance of genetic contributions to Ch gallstone disease.

The inbred mouse, with its superior genetic resources (18), is an excellent animal model (19, 20) for investigating genetic determinants of Ch cholelithiasis. In

Abbreviations: ACh, anhydrous cholesterol; BS, bile salt; Ch, cholesterol; ChM, cholesterol monohydrate; CSI, cholesterol saturation index; HPLC, high performance liquid chromatography; L, lecithin; TC, taurocholate; TCDC, taurochenodeoxycholate; TDC, taurodeoxycholate; T-β-MC, tauro-β-muricholate; T-ω-MC, tauro-ω-muricholate; TUDC, tauroursodeoxycholate.

[1]This paper was presented in part at Annual Meetings of the American Association for the Study of Liver Diseases, Chicago, IL, 1995, and the American Gastroenterological Association, San Francisco, CA, 1996, and published in abstract form in *Hepatology*. 1995. **22:** 289A and *Gastroenterology*. 1996. **110:** A1357, respectively.

[2]To whom correspondence should be addressed.

1964, Tepperman, Caldwell, and Tepperman (21) induced Ch gallstones in mice by feeding a lithogenic diet containing 1% Ch and 0.5% cholic acid, and discovered that mouse strains differed considerably in susceptibility. Later, Fujihira, Kaneta, and Ohshima (22) found that prevalence of Ch gallstones varied from 0 to 100% among six inbred strains of laboratory mice. Dueland et al. (23) reported that feeding a taurocholate (TC)-containing diet for 6 wks caused enlarged gallbladders and Ch gallstone formation in C57BL/6 mice, but not in BALB/c mice. Recently, we (24) studied 9 strains of inbred mice on a lithogenic diet and found that differences in gallstone susceptibility between C57L and AKR strains were determined by at least two *Lith* genes with *Lith1* mapping to mouse chromosome 2 by quantitative trait loci (QTL) analysis. These findings, taken together with the epidemiology of human cholelithiasis, point to genetic factors as playing a critical role in the development of Ch gallstone disease.

In the present study, we report the gallbladder phenotypes of *Lith* genes with particular reference to the physical-chemistry of bile in inbred mice with susceptible (C57L strain) and resistant (AKR strain) alleles. On the basis of the heterozygous phenotype in C57L X AKR (F_1) mice, we established the dominant inheritance of Ch gallstones. We also explored how genetic and dietary factors interacted to determine the incidence of Ch gallstones in each strain. These physical-chemical phenotypes provide a basic framework for investigating candidate *Lith* genes affecting Ch gallstone formation in this animal model.

MATERIALS AND METHODS

Chemicals

High performance liquid chromatographic (HPLC) grade reagents were obtained from Fisher Scientific Co. (Fair Lawn, NJ). BS standards were purchased from Sigma Chemical Co. (St. Louis, MO), and CalBiochem-Behring (San Diego, CA), with the exception of the taurine conjugates of α-, β-, and ω-muricholates (3α,6β,7α-trihydroxy-5β-cholanoate, 3α,6β,7β-trihydroxy-5β-cholanoate (T-β-MC), and 3α,6α,7β-trihydroxy-5β-cholanoate (T-ω-MC), respectively), which were generous gifts from Tokyo Tanabe Co., Tokyo, Japan (courtesy of Mr. H. Sugata). Purity of individual BS was at least >98% by HPLC (25, 26). All other chemicals and solvents were American Chemical Society or reagent grade quality (Fisher Scientific Co., Medford, MA).

Animals and diets

Homozygous C57L/J, AKR/J, and heterozygous (C57L × AKR) F_1 (24) mice of both genders, 4–6 wks old, were bred at The Jackson Laboratory, Bar Harbor, ME. (**Panel 1**) All animals were housed in a temperature-controlled room (22 ± 1°C) with a 12-h light cycle (6 AM–6 PM). Mice were provided free access to water and food (normal mouse chow or lithogenic diet) throughout the experimental period and were allowed to adapt to the environment for at least 2 wks prior to study. Normal Purina mouse chow contains trace Ch (The Mouse Diet 1401, St. Louis, MO 63144). Each 100 g of the semisynthetic lithogenic diet (24, 27) contains 15 g butter fat, 1 g Ch, 0.5 g cholic acid, 2 g corn oil, 50 g sucrose, 20 g casein, and essential vitamins and minerals. Biliary tract surgery was performed at 9 AM before (day 0) and at frequent intervals after feeding the lithogenic diet for 1 to 56 days. All experiments were executed according to accepted criteria for the care and use of laboratory animals. Protocols were approved by the Institutional Animal Care and Use Committee of Harvard University and were consistent with euthanasia recommendations of the American Veterinary Medical Association.

Collection of gallbladder biles and gallstones

Animals were fasted overnight but had free access to water. After weighing, mice were anesthetized with 35 mg/kg pentobarbital (Abbott Laboratories, North Chicago, IL) injected i.p. Under sterile conditions, laparotomy was performed through an upper midline incision. The liver and the gallbladder were examined, and gallstones and mucin gel, invariably visible through the gallbladder wall, were noted. The cystic duct was identified and doubly ligated, and a cholecystectomy was performed. Gallbladder volume was determined by *i*) immersion of the gallbladder into a partly filled 1-ml syringe and measuring water displacement, or *ii*) weighing the whole gallbladder and equating gallbladder weight (including stones when present) with gallbladder volume (24). To obtain sufficient bile volumes for lipid analyses, gallbladder contents were pooled from 30 C57L and F_1 mice and 40 AKR mice at each time point and frozen at −20°C. For quantitation of gallstone number, size, and Ch content, the gallbladder of each mouse was opened freshly and the inner surface was exposed. Using a polarizing light microscope (Photomicroscope III; Carl Zeiss Inc., Thornwood, NY), gallstones were counted at 200 × magnification and their diameters were measured with microscopic calipers. At 56 days, Ch content of 10–15 gallstones from each mouse strain was assayed by HPLC as described (28).

Panel 1. Photograph of three adult inbred mice with different susceptibilities to cholesterol gallstones. The mouse with "leaden-colored" coat (left) of C57L/J strain is homozygous for *Lith* genes. The white mouse (center) is AKR/J strain and has resistant *Lith* genes, and the black mouse (right) is the heterozygous (C57L×AKR)F_1 cross.

Microscopic studies

Fresh gallbladder bile was examined immediately after cholecystectomy according to methods described previously (25, 28). In brief, a 5-μL sample was placed on a glass slide at room temperature (≈22 ± 1°C) and observed without a cover slip (29) using the polarizing light microscope. The sample was then compressed with a cover glass and re-examined using phase contrast optics. To study the early stages of gallstone formation, a small hole was made with a 18-gauge needle at the fundus of the gallbladder. Bulk gallbladder bile dribbled by gravity through the small hole, and mucin gel was pressed out digitally with the assistance of a 24-gauge needle. Bulk and gel bile were examined separately by polarizing light microscopy for the presence of mucin strands, liquid and solid crystals, and sandy and true gallstones (see definition below) (24, 25, 28). In the late stages of gallstone formation, most of the gallbladder was filled with mucin gel, so that only a small portion of well-mixed bulk plus gel bile could be sampled for microscopic analysis. All phase separations were documented by 35 mm photography. Mucin was observed as non-birefringent amorphous strands, and verified by periodic acid/Schiff (PAS) staining (30). Arc, filamentous, tubular crystals (assumed to be metastable transitional forms of anhydrous Ch being hydrated to Ch monohydrate (ChM) crystals), ChM crystals as well as small, aggregated, and fused liquid crystals were defined according to previous criteria (25, 28). Sandy stones were irregularly shaped, and easily disintegrable agglomerates of ChM crystals embedded in mucin gel. As visualized under the microscope, individual flat Ch crystals projected clearly from their edges, and grossly they displayed a yellow color. True gallstones were hard, ball-like objects, and light yellow in color with smooth curved surfaces (21, 24). Because of scattered and absorbed light, they were opaque, and black in color under the microscope.

Lipid analyses

Biliary phospholipid was measured as inorganic phosphorus by the method of Bartlett (31). Ch was determined using an enzymatic assay (32). Total BS concentration was measured enzymatically by the 3α-hydroxysteroid dehydrogenase method (33). Individual BS were measured by HPLC according to the methods of Rossi, Converse, and Hofmann (34). Gallstones were washed, air-dried at 22°C, and the Ch content (wt/wt) was determined by HPLC (24, 35). Ch saturation indexes (CSI) of pooled biles were calculated from critical tables (36) established for TC, the predominant BS in mouse bile on the lithogenic diet (see later). Relative lipid compositions were plotted on condensed phase diagrams (28) according to the mean biliary lipid concen-

trations for mouse strain and gender. For graphic analysis, the phase limits of the micellar zones and the crystallization pathways were extrapolated from model systems developed for TC at 37°C (25, 37).

Statistical methods

All data are expressed as means ± SD. Differences among strains and outcrosses were assessed for statistical significances by the Student's *t*-test or chi-square test. Statistical significance was defined as a two-tailed probability less than 0.05.

RESULTS

Body weight

As expected for healthy rodents, mice of each strain showed progressive weight gain from 20–30 g to 27–38 g over the 56-day lithogenic diet feeding period. Males were appreciably (≈17–20%) heavier than females, and mice of strain AKR were ≈15–19% heavier than C57L and F_1 mice, which were identical to each other. All animals appeared healthy with the exception of 8 AKR mice (5%). These developed evidence of anorexia, lethargy, sleepiness, and weight loss, dying eventually between 42 and 50 days. At autopsy, no special causes of death relevant to the hepato-biliary system were found.

Macroscopic and microscopic observations: habits of solid and liquid crystals

At time 0, macroscopic and light microscopic examination of gallbladder biles showed no evidence of mucin gel, solid and liquid crystals, or gallstones. The gallbladder wall was thin and transparent, and gallbladder mucosa was smooth and cream to light red in color.

Figure 1 (a–l) displays photomicrographs of mucin strands, habits of solid Ch crystals, and optical textures of liquid crystals and gallstones. Mucin gel appeared as non-birefringent amorphous strands (Fig. 1a). Liquid crystals (25, 28) were denoted as small (Fig. 1b), when minimally sized, non-birefringent, and scattered; aggregated (Fig. 1c), when non-birefringent with particles of 1–5 μm diameter; and fused (Fig. 1d), when birefringent with focal conic Maltese-cross textures and greater than 0.5–1 μm in size (25, 28). In male C57L and F_1 mice, we found arc-like crystals infrequently (Fig. 1e). These were short curved rods (25, 28) and rarely were filamentous in habit (Fig. 1f). Tubular crystals (25, 28, 29) were detected only in biles of C57L and F_1 mice, and often appeared to fracture at their ends (Fig. 1g) producing plate-like ChM crystals (Fig. 1h). ChM crystals (Fig. 1h), typical of those seen in model (25) and human (28) biles and in human Ch gallstones (38), were 79.2° and 100.8° angled parallelograms, often with a small notched corner (38, 39). Amorphous masses of ChM crystal are defined loosely as agglomerated sheets (Fig. 1i). Sandy stones (Fig. 1j and k) were surrounded by mucin gel and exhibited individual ChM crystals projecting from their edges. Figure 1l shows true gallstones with typical round contours (21, 24) and black centers.

Ch crystallization sequences and gallstone formation

Table 1 enumerates all crystallization sequences and **Fig. 2** demonstrates selective aspects of the data to illustrate the evolution of Ch crystallization and gallstone formation according to gender in each mouse strain.

Male C57L mice (Fig. 2, top left panel). At 3 days, a layer of mucin gel adherent to the gallbladder wall was observed in all mice. By 5 days, some small scattered liquid crystals as well as ChM, arc, and tubular crystals were found principally in bulk bile. We observed small liquid crystals more frequently within mucin gel, suggesting a speedier evolution of crystallization. Occasionally, we detected filamentous or needle-shaped crystals principally within gelled bile. Numbers of solid and liquid crystals increased appreciably over the next 4 days, and aggregated liquid crystals formed. Principally, the high concentration of aggregated and fused liquid crystals (Fig. 1d) were most impressive within mucin gel. By 7 days (Fig. 2), 43% of mice had formed arc (presumed to be ACh), filamentous and/or tubular crystals (see Fig. 1(e–g)) that decreased by 14 days and, by 21 days, had vanished completely. With passage of time, individual ChM crystals enlarged in size and were consolidated by mucin gel as agglomerates 1–5 μm diameter. In contrast to mucin gel, bulk bile had a very weak reaction to PAS staining (30). By 21 days (Fig. 2), bile became turbid and contained some ball-shaped masses of agglomerated ChM crystals of various sizes (mostly ≤ 1 mm). Some crystal agglomerates floated freely, but the majority were implanted within mucin gel. At this time, many soft, fragile, and disintegrable sandy stones (see Fig. 1(j,k)) were detected. After 28 days (Fig. 2), 27%, and by 56 days, 80% of male C57L mice had formed true gallstones.

Female C57L mice (Fig. 2, top right panel). After 5 days of feeding, a layer of mucin gel became visible by direct light microscopy on the gallbladder mucosa. At 7 days (Fig. 2) small liquid crystals were detected in bulk bile as well as in mucin gel. Numbers of aggregated and fused liquid crystals increased progressively with time up to 7 and 14 days. At the same time, we found numerous ChM crystals of different sizes in both bulk bile and mucin gel. By 21 days (Fig. 2), large numbers of ChM as well as aggregated and fused liquid crystals were present. By

28 days, 6–10% of female C57L mice had formed sandy stones mainly within mucin gel; and by 56 days, 40% of mice had formed true gallstones.

Male and female F_1 mice (Fig. 2, middle panels). F_1 mice of either gender had identical evolutionary sequences of Ch crystallization and gallstone formation as described above for male and female C57L mice. In 33% of male F_1 mice, ACh crystals were detected between 7 and 21 days (Fig. 2) mirroring the affected male C57L parent. By 28 days, sandy stones were detected and gallstones had formed in 30% of male and 13% of female mice. By 56 days (Fig. 2), 77% of male and 33% of female mice had formed gallstones.

Male and female AKR mice (Fig. 2, bottom panels). At time 0, gallbladder biles of AKR mice were isotropic by polarizing light microscopy and were macroscopically light-yellow in color. By 14 days (Fig. 2), a thin layer of mucin gel was observed adherent to the gallbladder wall in 35% of mice. Mucin gel was invariably thinner in AKR mice by up to threefold compared with C57L mice. At 21 days (Fig. 2), small liquid crystals were detected in bulk bile as well as in mucin gel, and at later time points formed small aggregates. We detected some ChM crystals in both bulk bile and mucin gel at 37 days, and by 46 days, 5–8% of AKR mice had formed both sandy and true gallstones. At 56 days, gallstones had formed in 15% male and 13% female AKR mice. In contrast to C57L mice, the biliary phenotypes of AKR mice revealed no obvious gender difference, and no ACh crystals were detected.

Biliary lipid compositions and CSI during gallstone formation

Table 2 tabulates all gallbladder bile lipid compositions on chow (day 0) as well as on the lithogenic diet for 56 days. All mice had unsaturated gallbladder biles at time 0 that became Ch supersaturated gradually or rapidly depending upon strain and gender. As inferred from relative or absolute lipid compositions (25, 37), an increase in Ch content of bile occurred and became exaggerated with passage of time. Furthermore, all Ch/BS ratios showed significant increases from 0.03 ± 0.00 (day 0) to 0.13 ± 0.01 (56 days) in C57L and F_1 mice, and in AKR mice from 0.02 ± 0.00 (day 0) to 0.14 ± 0.01 (56 days), respectively. Also in C57L and F_1 mice, Ch/L ratios increased significantly from 0.21 ± 0.02 (day 0) to 0.49 ± 0.03 (56 days), and from 0.20 ± 0.01 (day 0) to 0.46 ± 0.01 (56 days) in AKR mice, respectively. As expected, when bile became most enriched in Ch (56 days), L/BS molar ratios were maximally increased (Table 2). These values ranged from 0.12 ± 0.02 (0 day) to 0.26 ± 0.01 in C57L, from 0.12 ± 0.01 to 0.27 ± 0.01 in F_1, and from 0.12 ± 0.00 to 0.30 ± 0.00 in AKR mice. These findings show that the lithogenic diet mainly increased the Ch as well as L concentrations of mouse gallbladder bile, and that solubility and phase separations of Ch were critically dependent on L/BS ratio and Ch concentration (Table 2). With respect to the solubilizing components of bile, Ch precipitation and growth into gallstones were predictable (36, 40–42) from the solubility relationships with respect to absolute and relative BS and L compositions as inferred from model systems.

Figure 3 displays the time-dependent changes in CSI that differed profoundly in the three mouse strains. CSI values of gallbladder bile in C57L and F_1 mice reached supersaturation at 1–2 wks and gradually increased to CSI = 1.3–1.5 by 56 days. In contrast, CSI values of AKR mice remained unsaturated for 28 days and then reached supersaturation abruptly at 37 days, whereafter CSI values increased to CSI = 1.2–1.3. CSI values for bile of F_1 mice and C57L mice were significantly higher than those of AKR mice ($P < 0.01$). Males of all strains invariably displayed higher CSI values and reached supersaturation earlier than females. As Table 2 shows, although total lipid concentration was significantly ($P < 0.01$) higher in AKR mice (means = 12.0 g/dL, males, and 13.7 g/dL, females) than in C57L (7.4 g/dL, males, and 9.2 g/dL, females) and F_1 mice (9.1 g/dL, males, and 9.0 g/dL, females), we did not find any appreciable change within each strain or gender over 56 days.

For purposes of illustration, we plot on triangular coordinates in **Fig. 4** the mean relative lipid compositions of gallbladder biles (Table 2) with micellar phase boundaries (37) and Ch crystallization pathways (25) for the appropriate mean total lipid concentrations in TC-rich bile. Figure 4 demonstrates that with duration of lithogenic diet feeding the relative lipid compositions of gallbladder biles progressively shifted upward and to the right of the phase diagrams. This shift was caused by an absolute and relative increases in Ch content, a relative increase in L content, and a relative decrease in BS content (Table 2). In C57L and F_1 mice, the biliary lipid compositions at 0, 1, 3, and 5 days plotted within the one-phase micellar zones, whereas after 7–14 days lipid compositions plotted above the micellar zone. By phase analysis, these biles were predicted to be composed of two or three phases, namely micellar bile, solid Ch crystals, and/or liquid crystals, exactly as was observed experimentally (Fig. 2). Because in male C57L and F_1 mice between 7 and 14 days the relative lipid composition of gallbladder bile passed through crystallization pathway B (25, 28), ACh crystals (arc, filamentous, and tubular crystals) appeared after ChM crystals (25) (Fig. 4). This phenomenon was also found by us to occur in a small number of human gallbladder biles (28). In contrast, during lithogenesis, the

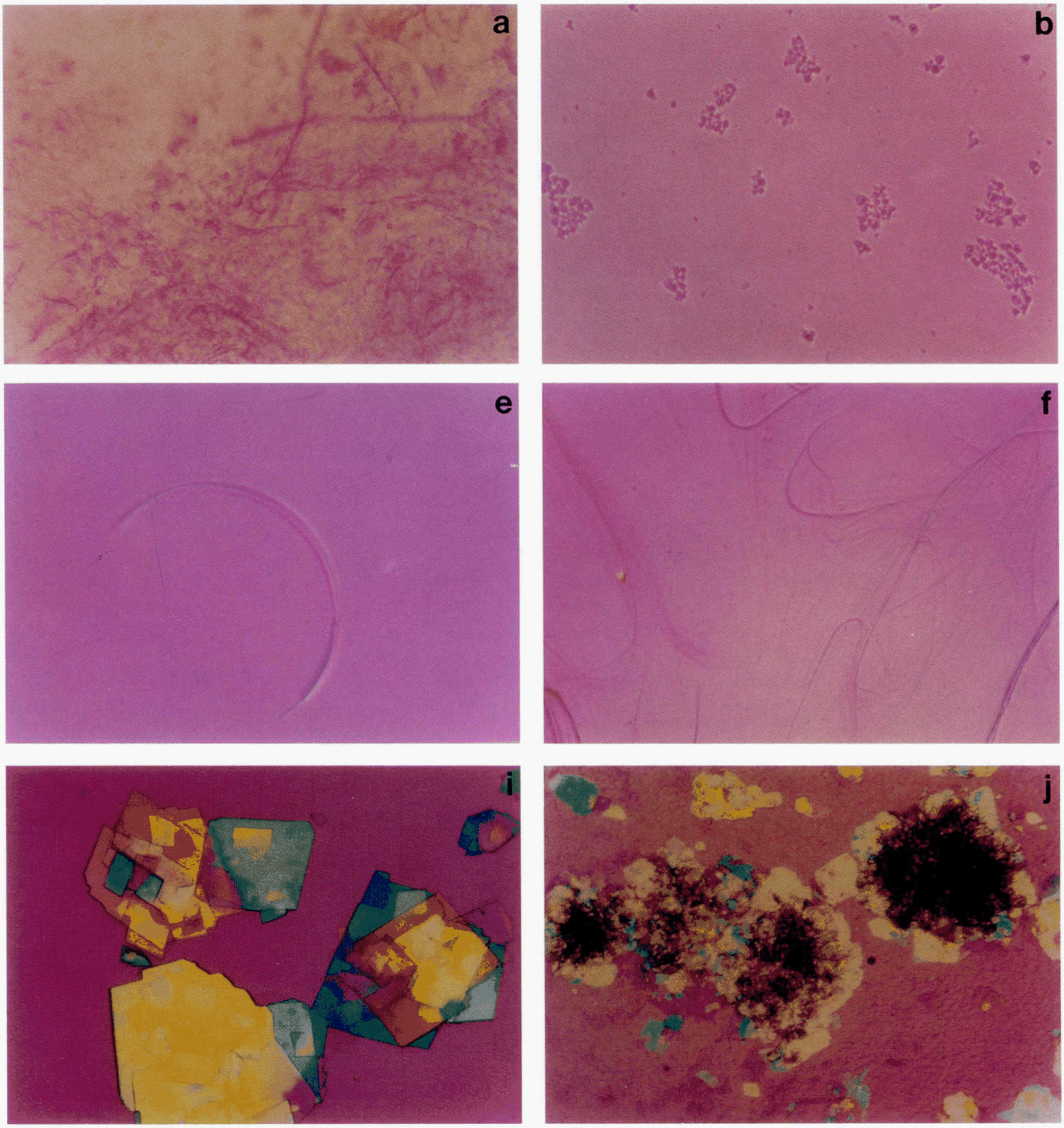

Fig. 1. Photomicrographs of mucin gel as well as habits of solid and liquid crystals, sandy stones, and true gallstones observed in C57L and F_1 males: (a) non-birefringent amorphous mucin gel; (b) small non-birefringent liquid crystals; (c) aggregated non-birefringent liquid crystals; (d) fused liquid crystals with Maltese-cross birefringence and focal conic textures; (e) arc-like (possible anhydrous Ch) crystal; (f) filamentous crystals; (g) tubular crystal fracturing at ends to produce plate-like ChM crystals with notched corners; (h) typical ChM crystal, with 79.2° and 100.8° angles; (i) agglomerated ChM crystals; (j and k) disintegratable amorphous sandy stones surrounded by mucin gel, with individual Ch crystals projecting from the edges; (l) gallstones exhibiting rounded contours and black centers from light scattering/absorption. All magnifications × 1600 except Fig. 1j, × 800; and Fig. 1(k and l), × 400 by polarizing light microscopy.

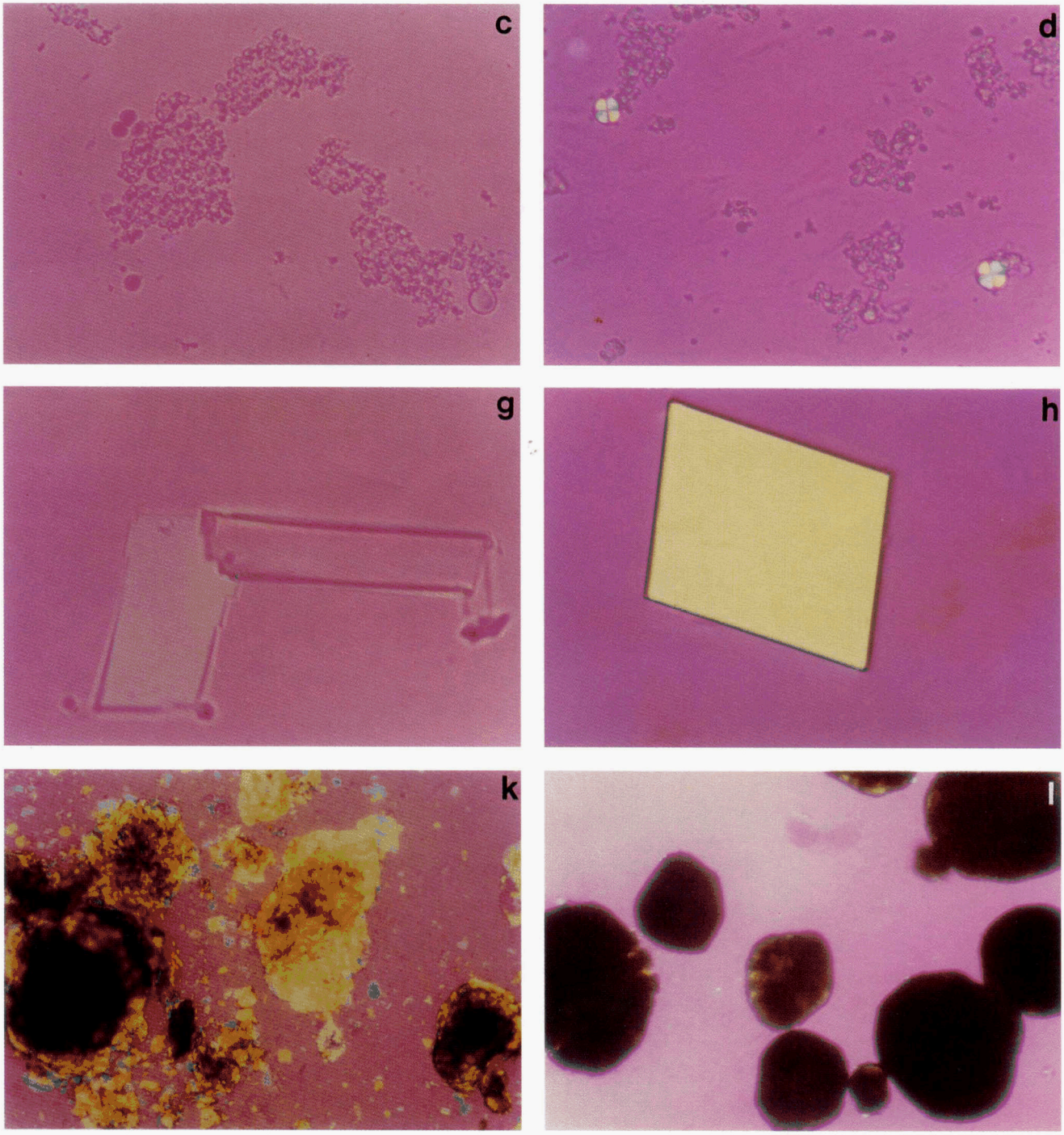

Fig. 1.

relative lipid compositions of gallbladder bile in female C57L, F_1, and male and female AKR mice entered crystallization pathway C from the one-phase micellar zone (Fig. 4). Therefore, we did not find ACh crystals in these biles (25). It is notable (Fig. 4) that during Ch supersaturation, the relative lipid compositions of gallbladder biles of AKR mice entered region C abruptly from an unsaturated micellar state that lasted more than two weeks (Fig. 3). Accordingly, as predicted from model systems (25), liquid crystals invariably proceeded ChM crystals during crystallization (Fig. 2).

Effects of lithogenic diet on gallbladder sizes

Figure 5 displays mouse gallbladder sizes (μL) as functions of days on the lithogenic diet. Before feeding the lithogenic diet (day 0), gallbladders of C57L and F_1

TABLE 1. Crystallization sequences in gallbladder biles

	Males										Females									
Day	Mucus	Arc	Filament	Tubule	ChM	SLC	ALC	FLC	SS	GS	Mucus	Arc	Filament	Tubule	ChM	SLC	ALC	FLC	SS	GS
C57L																				
0	0/30	0/30	0/30	0/30	0/30	0/30	0/30	0/30	0/30	0/30	0/30	0/30	0/30	0/30	0/30	0/30	0/30	0/30	0/30	0/30
1	0/30	0/30	0/30	0/30	0/30	0/30	0/30	0/30	0/30	0/30	0/30	0/30	0/30	0/30	0/30	0/30	0/30	0/30	0/30	0/30
3	13/30	0/30	0/30	0/30	0/30	0/30	0/30	0/30	0/30	0/30	0/30	0/30	0/30	0/30	0/30	0/30	0/30	0/30	0/30	0/30
5	25/30	2/30	1/30	3/30	14/30	10/30	5/30	2/30	0/30	0/30	12/30	0/30	0/30	0/30	0/30	0/30	0/30	0/30	0/30	0/30
7	30/30	10/30	3/30	13/30	30/30	11/30	2/30	1/30	0/30	0/30	17/30	0/30	0/30	0/30	0/30	11/30	0/30	0/30	0/30	0/30
9	30/30	3/30	2/30	5/30	30/30	23/30	10/30	5/30	0/30	0/30	30/30	0/30	0/30	0/30	0/30	18/30	4/30	1/30	0/30	0/30
14	30/30	2/30	0/30	3/30	30/30	26/30	13/30	8/30	0/30	0/30	30/30	0/30	0/30	0/30	0/30	7/30	19/30	3/30	3/30	0/30
21	30/30	0/30	0/30	0/30	30/30	21/30	18/30	7/30	2/30	0/30	30/30	0/30	0/30	0/30	18/30	26/30	7/30	5/30	0/30	0/30
28	30/30	0/30	0/30	0/30	30/30	22/30	11/30	5/30	4/30	8/30	30/30	0/30	0/30	0/30	21/30	30/30	13/30	13/30	3/30	2/30
56	30/30	0/30	0/30	0/30	30/30	23/30	23/30	12/30	7/30	24/30	30/30	0/30	0/30	0/30	29/30	30/30	13/30	13/30	9/30	12/30
F_1																				
0	0/30	0/30	0/30	0/30	0/30	0/30	0/30	0/30	0/30	0/30	0/30	0/30	0/30	0/30	0/30	0/30	0/30	0/30	0/30	0/30
1	0/30	0/30	0/30	0/30	0/30	0/30	0/30	0/30	0/30	0/30	0/30	0/30	0/30	0/30	0/30	0/30	0/30	0/30	0/30	0/30
5	18/30	4/30	1/30	2/30	11/30	11/30	5/30	2/30	0/30	0/30	9/30	0/30	0/30	0/30	0/30	3/30	0/30	0/30	0/30	0/30
7	22/30	1/30	3/30	10/30	18/30	16/30	8/30	3/30	0/30	0/30	19/30	0/30	0/30	0/30	0/30	13/30	1/30	0/30	0/30	0/30
14	30/30	2/30	0/30	3/30	30/30	17/30	10/30	7/30	0/30	0/30	30/30	0/30	0/30	0/30	9/30	16/30	4/30	2/30	0/30	0/30
21	30/30	0/30	0/30	0/30	30/30	22/30	14/30	7/30	0/30	0/30	30/30	0/30	0/30	0/30	21/30	23/30	10/30	5/30	0/30	0/30
28	30/30	0/30	0/30	0/30	30/30	24/30	10/30	8/30	5/30	9/30	30/30	0/30	0/30	0/30	30/30	27/30	15/30	10/30	3/30	4/30
56	30/30	0/30	0/30	0/30	30/30	25/30	13/30	9/30	6/30	23/30	30/30	0/30	0/30	0/30	27/30	25/30	21/30	9/30	8/30	10/30
AKR																				
0	0/40	0/40	0/40	0/40	0/40	0/40	0/40	0/40	0/40	0/40	0/40	0/40	0/40	0/40	0/40	0/40	0/40	0/40	0/40	0/40
1	0/40	0/40	0/40	0/40	0/40	0/40	0/40	0/40	0/40	0/40	0/40	0/40	0/40	0/40	0/40	0/40	0/40	0/40	0/40	0/40
3	0/40	0/40	0/40	0/40	0/40	0/40	0/40	0/40	0/40	0/40	0/40	0/40	0/40	0/40	0/40	0/40	0/40	0/40	0/40	0/40
5	0/40	0/40	0/40	0/40	0/40	0/40	0/40	0/40	0/40	0/40	0/40	0/40	0/40	0/40	0/40	0/40	0/40	0/40	0/40	0/40
7	0/40	0/40	0/40	0/40	0/40	0/40	0/40	0/40	0/40	0/40	0/40	0/40	0/40	0/40	0/40	0/40	0/40	0/40	0/40	0/40
9	0/40	0/40	0/40	0/40	0/40	0/40	0/40	0/40	0/40	0/40	0/40	0/40	0/40	0/40	0/40	0/40	0/40	0/40	0/40	0/40
14	14/40	0/40	0/40	0/40	0/40	0/40	0/40	0/40	0/40	0/40	18/40	0/40	0/40	0/40	0/40	0/40	0/40	0/40	0/40	0/40
21	27/40	0/40	0/40	0/40	0/40	18/40	5/40	3/40	0/40	0/40	30/40	0/40	0/40	0/40	0/40	25/40	4/40	1/40	0/40	0/40
28	25/40	0/40	0/40	0/40	0/40	13/40	8/40	6/40	0/40	0/40	33/40	0/40	0/40	0/40	0/40	23/40	3/40	1/40	0/40	0/40
37	34/40	0/40	0/40	0/40	16/40	25/40	19/40	9/40	0/40	0/40	35/40	0/40	0/40	0/40	14/40	26/40	10/40	6/40	0/40	0/40
46	38/40	0/40	0/40	0/40	23/40	28/40	16/40	7/40	2/40	3/40	35/40	0/40	0/40	0/40	20/40	28/40	17/40	9/40	2/40	3/40
56	38/40	0/40	0/40	0/40	36/40	32/40	19/40	9/40	7/40	6/40	38/40	0/40	0/40	0/40	32/40	30/40	24/40	10/40	4/40	5/40

Values are expressed as the number of mice forming mucus, solid and liquid crystals, and gallstones to total number of mice examined at each time point. Abbreviations: ChM, cholesterol monohydrate crystals; SLC, small liquid crystals; ALC, aggregated liquid crystals; FLC, fused liquid crystals; SS, sandy stones; GS, real gallstones (see text for defintions).

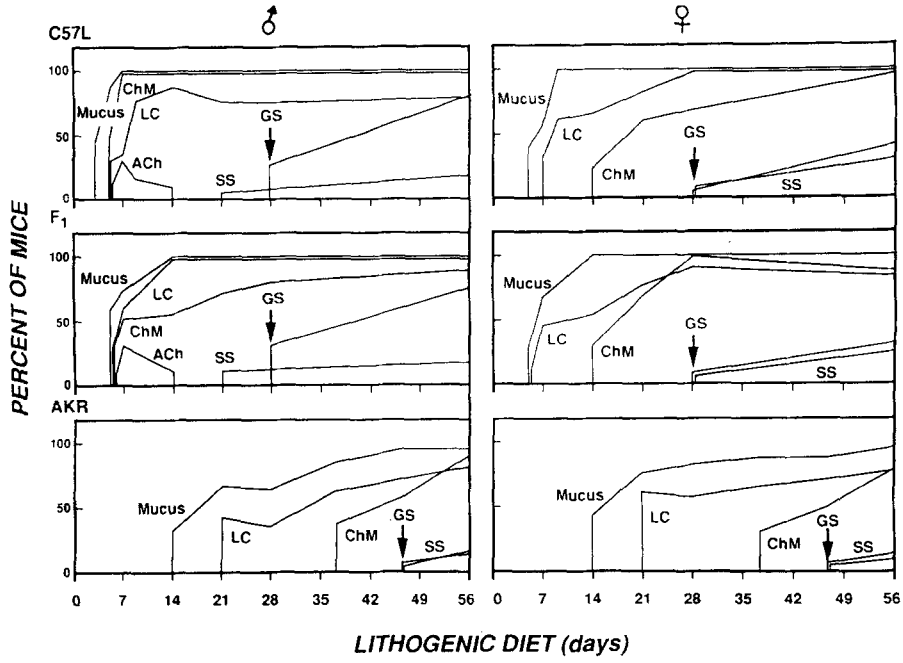

Fig. 2. Percent of mice forming mucin gel, solid and liquid crystals (multilamellar vesicles), sandy stones, and true gallstones as functions of days on the lithogenic diet. The panels show the time sequences as means for each group of inbred mice. Arrows indicate the first appearances of true gallstones (see Fig. 11). Abbreviations: ACh, anhydrous cholesterol crystals, including arc-like, filamentous as well as transitional tubular crystals; ChM, cholesterol monohydrate crystals; LC, liquid crystals, including small, aggregated and fused (multilamellar) varieties; SS, sandy stones; GS, true gallstones. (See text for further description.)

mice were approximately double the sizes in AKR mice. Response of the gallbladders in C57L, F_1, or AKR mice did not differ up to 28 days of lithogenic diet feeding. However, in C57L and F_1 mice, gallbladder size increased slightly after 28 days when Ch crystallization and gallstones were fully developed (Fig. 2). This increase in gallbladder size paralleled the elevated CSIs in bile, and both were much more marked in C57L mice compared with AKR mice. Furthermore, gallbladder sizes were significantly larger in female C57L, F_1, and AKR mice than in males ($P < 0.01$).

Molecular species of bile salts in gallbladder bile

Figure 6 displays the BS species determined by HPLC in gallbladder biles of mice before and during feeding the lithogenic diet. All BS species were taurine-conjugated, and while mice were on the chow diet they were similarly distributed in each strain and gender. Taurocholate (TC) (range 46–54%) and tauro-β-muricholate (T-β-MC) (range 34–42%) were the predominant BS species. Tauro-ω-muricholate (T-ω-MC) (2–5%), tauroursodeoxycholate (TUDC) (2–7%), taurochenodeoxycholate (TCDC) (1%), and taurodeoxycholate (TDC) (2–6%) were present in much smaller concentrations. With the lithogenic diet, TC in C57L and F_1 mouse biles increased markedly to 71–91% even after 1 day, and then decreased somewhat, remaining at 60–82% for the duration of the experiment. In contrast, over the same time period, T-β-MC decreased to 10–14%, and fell to 5% for the remainder of feeding. In the gallstone-susceptible C57L and F_1 strains, both TCDC and TDC increased sharply at day 5, and remained at 10–20% and 5–10% levels, respectively, for the duration of feeding. Further, both T-ω-MC and TUDC constituted minor bile salts and did not change with the length of feeding. In AKR mice, the lithogenic diet also resulted in an increase in TC to 70% which remained at approximately 53–80% after 1 day (Fig. 6). Reciprocally, T-β-MC decreased sharply on day 3 and then increased significantly to 13–26% thereafter. In bile of AKR mice after the first 2–3 days, the lithogenic diet produced no additional changes in percentages of T-ω-MC, TUDC, TCDC, or TDC.

Prevalence, chemistry, size and number of gallstones at 56 days

Figure 7 shows prevalence rates and average Ch gallstones diameters at 56 days. As indicated on the top panel, gallstone prevalence was identical in C57L and F_1 mice and was significantly greater than in AKR mice ($P < 0.01$). Moreover, gallstone prevalence rates were

TABLE 2. Biliary lipid compositions of gallbladder biles during gallstone formation

	Males						Females					
Day	Mole%Ch	Mole%L	Mole%BS	L/(L + BS)	[TL](g/dl)	CSI[a]	Mole%Ch	Mole%L	Mole%BS	L/(L+BS)	[TL](g/dl)	CSI[a]
C57L												
0	2.33	9.86	87.81	0.10	6.75	0.61	2.47	12.26	85.27	0.13	8.12	0.53
1	2.36	10.02	87.62	0.10	6.96	0.62	2.39	11.95	85.66	0.12	8.55	0.54
3	3.02	10.68	86.30	0.11	7.78	0.73	2.69	13.02	84.30	0.13	8.11	0.61
5	3.50	11.08	85.42	0.11	7.61	0.85	3.53	14.01	82.46	0.15	6.87	0.72
7	4.47	12.35	83.18	0.13	6.23	1.02	4.68	14.96	80.35	0.16	7.54	0.89
9	5.80	13.93	80.27	0.15	6.24	1.20	5.32	15.25	79.43	0.16	8.92	0.99
14	6.07	15.31	78.63	0.16	7.34	1.17	5.80	15.99	78.21	0.17	9.29	1.02
21	7.21	14.93	77.86	0.16	7.92	1.37	6.50	17.16	76.34	0.18	9.97	1.09
28	8.19	16.24	75.57	0.18	9.26	1.39	7.46	17.37	75.17	0.19	9.75	1.21
56	9.48	18.37	72.15	0.20	7.50	1.53	9.92	19.32	70.77	0.21	14.57	1.38
F_1												
0	2.24	11.14	86.62	0.11	9.73	0.50	2.17	10.67	87.16	0.11	8.73	0.51
1	3.05	11.47	85.48	0.12	6.79	0.72	2.68	12.70	84.62	0.13	8.91	0.57
5	4.06	12.10	83.85	0.13	8.58	0.89	3.44	13.98	82.59	0.15	8.65	0.69
7	4.29	12.84	82.87	0.13	9.46	0.88	3.89	14.74	81.37	0.15	9.93	0.72
14	6.90	14.18	78.92	0.15	9.33	1.32	6.01	16.07	77.92	0.17	8.73	1.07
21	7.22	14.96	77.83	0.16	8.88	1.34	7.03	17.02	75.94	0.18	8.94	1.18
28	7.03	16.79	76.18	0.18	9.94	1.18	7.78	18.22	74.01	0.20	7.94	1.26
56	9.22	19.58	71.20	0.22	10.08	1.36	9.02	20.01	70.98	0.22	9.94	1.32
AKR												
0	1.81	10.53	87.66	0.11	9.98	0.42	2.14	10.35	87.52	0.11	12.47	0.47
1	1.66	11.39	86.95	0.12	12.59	0.35	1.56	10.94	87.50	0.11	15.43	0.33
3	1.94	12.30	85.77	0.13	12.36	0.38	2.47	14.30	83.23	0.15	13.05	0.44
5	2.58	13.88	83.54	0.14	11.79	0.49	3.14	15.64	81.21	0.16	14.66	0.53
7	2.58	14.75	82.67	0.15	12.25	0.47	2.85	16.18	80.96	0.17	13.75	0.47
9	3.27	14.89	81.84	0.15	11.77	0.60	3.48	17.39	79.13	0.18	13.93	0.55
14	4.31	14.91	80.78	0.16	11.70	0.75	3.93	17.62	78.45	0.18	14.32	0.62
21	4.45	16.04	79.51	0.17	12.41	0.74	3.74	18.34	77.93	0.19	13.13	0.57
28	4.54	16.56	78.90	0.17	11.19	0.77	4.41	18.94	76.65	0.20	14.51	0.64
37	7.73	19.08	73.19	0.21	11.59	1.15	7.46	18.60	73.94	0.20	13.52	1.10
46	8.45	20.59	70.96	0.23	12.16	1.17	8.33	19.55	72.12	0.21	13.35	1.17
56	9.73	20.74	69.53	0.23	14.29	1.30	8.99	21.08	69.93	0.23	12.44	1.22

Values were determined from the pooled gallbladder biles. Abbreviations: Ch, cholesterol; L, lecithin; BS, bile salt; [TL], total lipid concentration; CSI, cholesterol saturation index.
[a]These values represent the mean CSI values of the pooled gallbladder biles calculated from the critical tables (36).

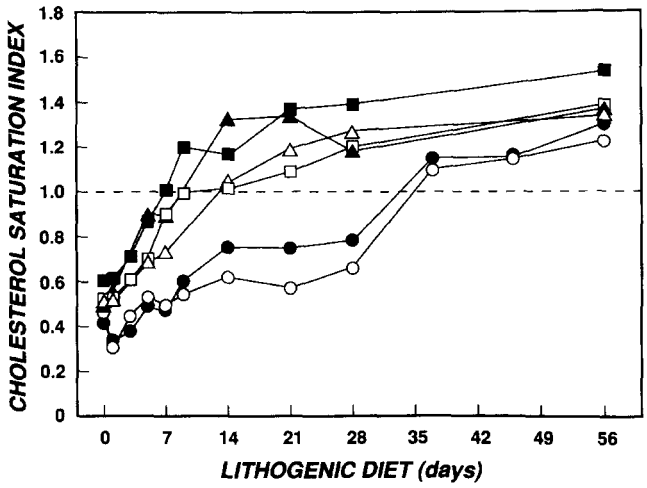

Fig. 3. CSI values of gallbladder bile as functions of mouse strain, gender, and time on the lithogenic diet. In C57L and F_1 mice, the CSI of gallbladder biles (pooled) reached supersaturation after 1 wk. In AKR mice, the CSI remained unsaturated up to 4 wks, and then became supersaturated abruptly between 4 and 5 wks. Symbol ■ represents male C57L, □ female C57L, ▲ male F_1, △ female F_1, ● male AKR, and ○ female AKR mice.

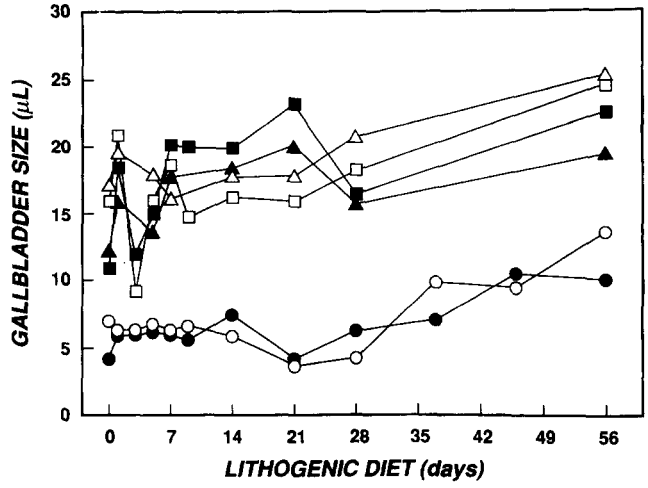

Fig. 5. Gallbladder sizes as functions of time on the lithogenic diet. The volumes were larger in C57L and F_1 mice than in AKR mice, but were similar between C57L and F_1 mice. Gallbladder sizes increased slightly over time in C57L and F_1 mice, whereas in AKR mice, they remained unchanged up to 28 days. At 56 days of lithogenic diet feeding, all mice displayed 1.5- to 2-fold increases (all NS) in gallbladder sizes. Symbol ■ represents male C57L, □ female C57L, ▲ male F_1, △ female F_1, ● male AKR, and ○ female AKR mice.

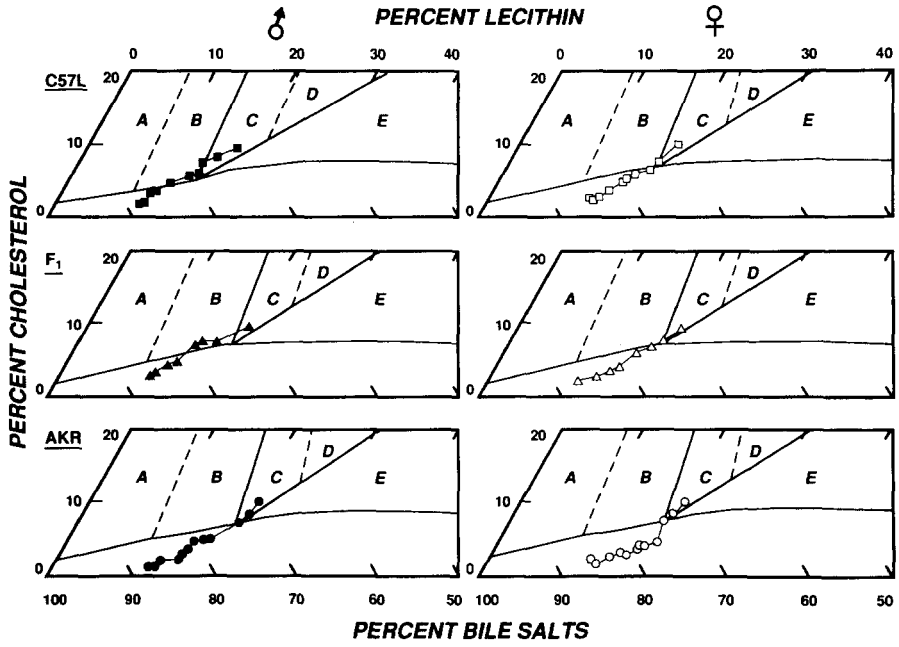

Fig. 4. Mean relative lipid compositions (moles per 100 moles) of gallbladder biles (pooled) at each time point plotted on condensed phase diagrams for average total lipid concentrations of the bile samples (from Table 2) which were 7.4 g/dL (males) and 9.2 g/dL (females) (C57L strain), 9.1 g/dL (males) and 9.0 g/dL (females) (F_1 strain), 12.0 g/dL (males) and 13.7 g/dL (females) (AKR strain). The one-phase micellar zone is enclosed by a solid curved line. Above the micellar zone, two solid and two dashed lines divide the phase diagrams into regions A to E with different crystallization sequences (see ref. 25). With passage of time, in all strains the relative lipid compositions of gallbladder bile shifted upward progressively and to the right. Only the lipid compositions of biles in C57L and F_1 males passed through region B. In contrast, the lipid compositions of bile in C57L and F_1 females as well as AKR mice entered crystallization pathway C directly from the one-phase micellar zone. Symbol ■ represents male C57L, □ female C57L, ▲ male F_1, △ female F_1, ● male AKR, and ○ female AKR mice. See text for further description.

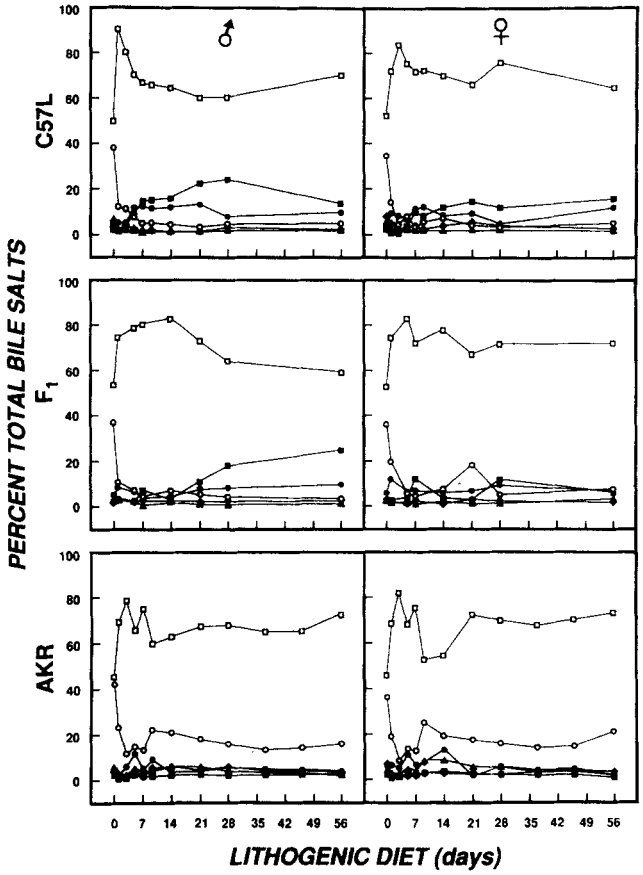

Fig. 6. Bile salt (BS) species as function of days on the lithogenic diet displayed as percent total BS. TC and T-β-MC (see list of abbreviations) were the predominant BS when mice were fed laboratory chow. Because the lithogenic diet contained 0.5% cholic acid, TC replaced most T-β-MC over the first few days in all strains of mice. In C57L and F_1 mice, percent of TCDC and TDC, more hydrophobic BS increased sharply at 5 days and remained elevated for the duration of feeding whereas the hydrophilic BS such as T-β-MC remained at ≈2%. In AKR mice, after the first few days the percent hydrophobic BS remained unchanged at 1–3% while the hydrophilic T-β-MC remained at ≈20%. Symbol □ represents TC; ○ T-β-MC; ■ TCDC; ● TDC; ▲ T-ω-MC; and ◆ TUDC. See text for further description.

2-fold higher in C57L and F_1 males than females ($P < 0.01$), but there were no gender differences in AKR mice (Fig. 7). The bottom panel of Fig. 7 shows that gallstone diameters in C57L (0.56 ± 0.31 mm) and F_1 (0.49 ± 0.26 mm) males were significantly ($P < 0.01$) bigger than in AKR (0.30 ± 0.09 mm) males, but the small differences among C57L (0.33 ± 0.12 mm), F_1 (0.31 ± 0.17 mm), and AKR (0.28 ± 0.11 mm) females did not reach significance.

Figure 8 shows the frequency distribution of gallstones at 56 days as functions of mouse strain and gender. On average, the number of gallstones in C57L and F_1 mice fell between 7 and 9, whereas in AKR mice the corresponding values were 4 and 6. Most notably, gallbladders of AKR mice displayed much lower gallstone numbers than in C57L and F_1 mice, and 85–88% of AKR mice were gallstone free.

The extracted sterols from all gallstones of each mouse strain contained only Ch, which constituted 95–99% of pooled stone weight.

DISCUSSION

Gallbladder bile phenotypes of *Lith* genes in inbred mice

The goal of the present studies was to define the gallstone and gallbladder bile phenotypes rigorously so as to provide a frame of reference in searching for possible candidate genes for gallstone susceptibility. The most important findings were: *i*) *Lith* genes were crucial in elevating CSI, speed of Ch crystal formation, gallbladder volume, and size and number of Ch gallstones. *ii*) As the F_1 phenotype mimicked the affected C57L parent, this confirmed that susceptibility to Ch gallstones was a dominant trait in the outcross. *iii*) A small percentage of AKR mice formed Ch gallstones after receiving the lithogenic diet for a much longer time period. As they did so abruptly and only in a small percentage of mice, this suggests an additional environmental factor such as severe hepatic steatosis (D. Q-H. Wang, J. M. Crawford, F. Lammert, B. Paigen, and M. C. Carey, unpublished observations) might contribute to the phenotype. *iv*) Besides the well-known liquid crystal to solid ChM crystal pathway in model and gallbladder biles (43), the direct ChM crystallization pathway and an ACh crystal to solid ChM crystal pathway (25, 29) also occurred in gallbladder biles but they differed among the lithogenic C57L, F_1, and AKR strains and genders. Therefore, in inbred mice, we identified three Ch crystallization pathways as part of the phenotypes of gallbladder bile, which were identical to those found in model biles for physiological lipid composition (25, 29) and in native human biles (28).

Physical-chemical characterization of gallbladder biles

Evolutionary sequences of Ch crystallization and gallstone formation were characterized by the initial accumulation of mucin gel, followed by appearances of liquid crystals and/or ACh crystals and ChM crystals, and then agglomerated ChM, sandy stones, and true gallstones, which were identical in appearance in all gallbladders. These sequences are in agreement with results of investigations in other animal models of Ch gallstone formation, such as the prairie dog (44, 45). Although this is not easily achieved in humans, investigators (46–49) have attempted to study the physical-chemical phase separation sequences in bile before and

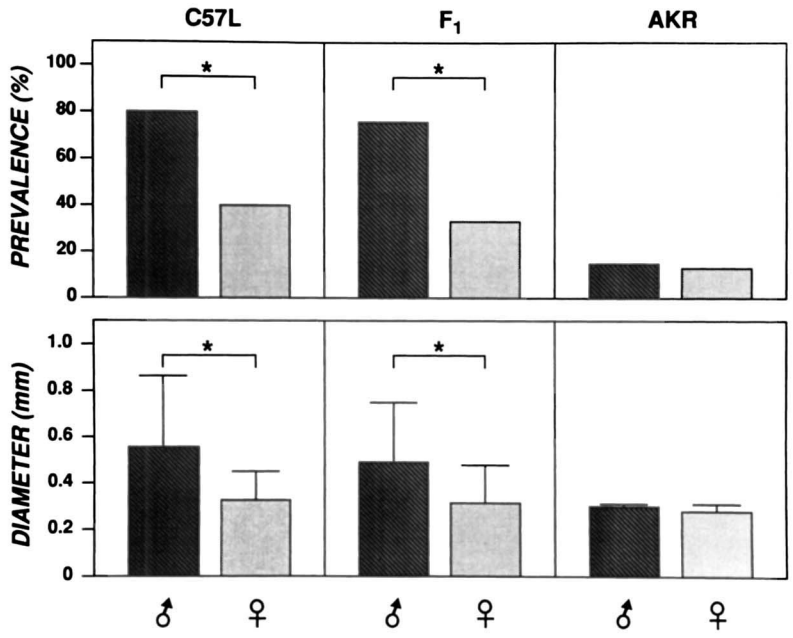

Fig. 7. Gallstone characteristics at 56 days. The top panel displays gallstone prevalence, and the bottom panel, gallstone diameters. Both prevalence and size were identical between C57L and F_1 mice, but were significantly greater in male C57L and F_1 mice than in females or AKR mice where the characteristics were independent of gender. Asterisks indicate $P < 0.01$.

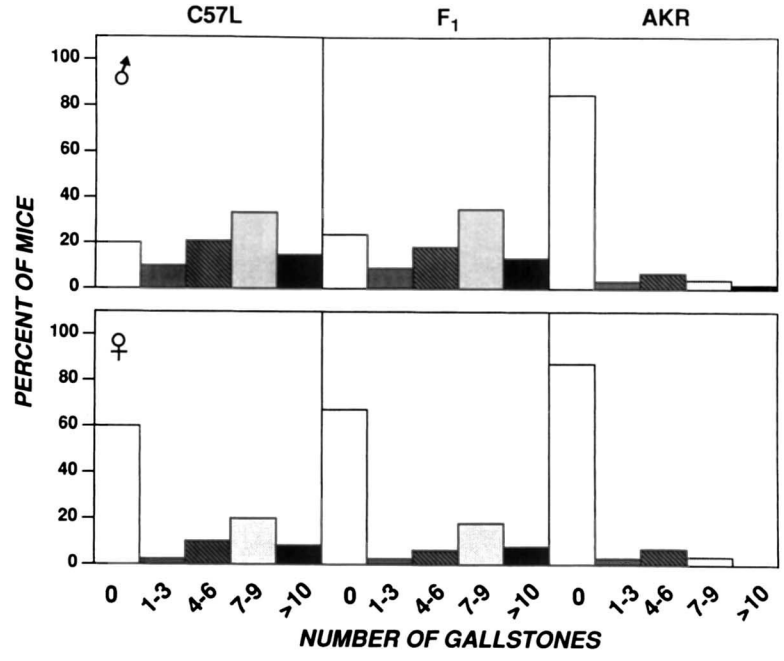

Fig. 8. Numbers of gallstones at 56 days. Gallbladders of both C57L and F_1 mice showed significantly higher gallstone numbers than in AKR mice. Most C57L and F_1 gallbladders contained between 7 and 9 gallstones, whereas AKR mice contained between 4 and 6. Note that the majority of AKR mice remained gallstone free.

during gallstone formation among obese patients who ingested a very low-calorie diet or were undergoing weight reduction after gastric-bypass surgery. These models of rapid Ch gallstone formation (46–49) indicated that CSI became elevated earliest, followed by dramatic increases in the concentration of mucin glycoproteins and ex vivo evidence of shortened ChM crystal detection times, and then in vivo ChM crystal formation. Finally, 37% of obese patients undergoing rapid weight loss had Ch gallstones or microstones by 19 wks (48). The substantial evidence from these human investigations is in accord with the results of the present study in inbred mice.

The following pathophysiological alterations might be responsible for accelerated Ch crystallization and gallstone formation observed in susceptible mice. First, the mean Ch content, i.e., CSI,[3] in pooled gallbladder

[3]T-β-MC, a poor Ch solubilizer (50) comprised 34–42% of BS in mouse gallbladder bile during chow feeding and the first 1–2 days of

biles increased rapidly after the lithogenic diet was initiated and reached supersaturation by 1–2 wks in C57L and F_1 mice. Second, marked gallbladder mucin accumulation occurred in C57L and F_1 mice fed the lithogenic diet for 3 days, that is, prior to the formation of solid crystals, liquid crystals and gallstones, and Ch crystals grew predominantly within mucin gel that accumulated first on the gallbladder wall. These sequences of biliary events are in agreement with earlier results of Alexander and Portman (19). Therefore, these observations suggest that the expression of mucin (*Muc*) genes (51) and mucin secretion in the gallbladder may be enhanced because of stimulation by some components such as increased levels of Ca^{2+}, BS, or ATP (52) in Ch supersaturated bile and/or the regulation of *Lith* genes. Third, our studies showed that the percent of hydrophobic BS such as TDC increased from 2–5% to 5–10% in C57L and F_1 mice concomitant with the early stages of lithogenic diet feeding. This is in agreement with observations in Ch gallstone patients (28, 53, 54) who usually have higher percentages of hydrophobic BS compared with controls. Studies on model (25, 55) and human biles (28, 54) have shown that increased levels of hydrophobic BS induced rapid Ch crystal precipitation, either because they induce more rapid aggregation and fusion of vesicles (56) or they shift crystallization pathways on phase diagrams to positions that favor Ch crystallization (25, 28). Fourth, the lower total lipid concentration in bile of C57L and F_1 mice could decrease the Ch-solubilizing capacity (25, 36, 37), favoring earlier formation of Ch-supersaturated bile (25, 57), and acceleration of gallstone formation. Finally, the bigger gallbladder sizes and larger volumes of mucin gel in C57L and F_1 mice might have enhanced Ch crystallization and gallstone formation compared with AKR mice. The motility of the gallbladders might be more impaired in the susceptible mice and this constitutes one of the trinity of cardinal pathophysiological defects, involved in Ch gallstone pathogenesis (1, 2). In fact, our ongoing study (58) of cholecystokinin (CCK)-A receptor-deficient mice fed a normal chow diet showed that the "knockout" mice had larger gallbladders and ablated gallbladder motility after an i.p. CCK bolus. When fed a lithogenic diet, these mice displayed markedly increased susceptibility to Ch gallstone formation at 12 wks (58).

The present work confirms that the ACh crystal to ChM crystal pathway (25, 29) also occurs in 30–43% male C57L and F_1 mice during Ch gallstone formation as it does in some humans (28). When the biliary compositions of these mice were plotted on phase diagrams, they passed through region B (Fig. 5) where ACh crystals separate from bile as was shown in model systems (25) and in some recrystallizing human biles (28). This explains not only the occurrence of ACh crystallization in male C57L and F_1 mice, but also provides a clue as to why CSIs reached supersaturation earlier in C57L and F_1 mice compared with AKR mice (see Fig. 3).

Candidate functions for *Lith* genes as inferred from gallbladder phenotypes

The current study suggests that several physiological functions could be altered to induce Ch gallstone formation. For example, the higher CSIs observed in gallstone-susceptible mice suggest that *Lith* gene products might increase Ch secretion from the liver (59). This might result from up-regulated Ch synthesis, increased Ch absorption, or defective disposition such as from reduced de novo BS synthesis and cholesteryl ester formation. All three could provide an important source of excess Ch molecules for secretion into hepatic bile thereby increasing its Ch content.

The principal enzymes of Ch metabolism that alter pools of free Ch within the liver are 3-hydroxy-3-methylglutaryl-CoA reductase (HMGR), acyl-CoA:cholesterol acyltransferase (ACAT) Ch 7α-hydroxylase (C7H), and sterol 27-hydroxylase (S27H). We assayed these enzymes during feeding the lithogenic diet (60) and have preliminary data confirming that HMGR regulation differs between C57L and AKR with the former resisting down-regulation by Ch (24). The structural genes for HMGR map to mouse chromosome 13 (61), ACAT to chromosome 1 (62), and S27H to chromosome 1 (63), respectively. As *Lith1* maps to chromosome 2, these enzymes themselves or their adjacent regulatory DNA such as promoter or binding sites for regulatory molecules could not account for the *Lith1* gene, simply because they map to the wrong chromosomes. However, differences in proteins that determine the concentrations of regulatory molecules remain possible candidate defects.

The second class of candidate genes that could affect Ch pools within the liver are Ch transport molecules. These might be low density lipoprotein receptor (LDLR) (64), the scavenger receptor SR-B1, i.e., high density lipoprotein receptor (HLDR) (65), and chylomicron remnant receptor(s) (66) that could transport Ch in plasma lipoproteins into liver cells, or sterol carrier protein 2 (SCP2) (67), which is believed to play an important role in intracellular lipid movement. Although structural genes for LDLR, HDLR, and SCP2 map to mouse chromosomes 9 (62, 68), 8 (62), and 4 (69), respectively, the proteins encoded by *Lith* genes might regulate their gene expression. Furthermore, it is possible that there is a protein in the bile canalicular membrane that could transport Ch molecules into or

the lithogenic diet. Therefore, the "urso-correction factor" (36) was used to calculate a more realistic assessment of the early CSIs. Based upon this adjustment, it is likely that over the first 3 days the "true" CSIs in gallbladder bile would approximate 0.80–1.10 in C57L and F_1 mice, and ≈0.80 in AKR mice.

out of hepatic bile. With respect to this possibility, it has been suggested (62) that megalin (Gp330) (70), a member of the *Ldlr* gene family, might be a possible candidate gene. It maps to the same region of the mouse chromosome 2 (70) as the *Lith1* gene (24). Moreover, prior to feeding the lithogenic diet there is identicalness of micellar BS species in the susceptible and resistant mouse strains, so that the physical-chemical aspects of intestinal Ch solubilization and absorption are equivalent (50, 71). Yet, the CSI of gallbladder bile in C57L mice was appreciably higher than in AKR mice (Fig. 3). Because hepatic HMGR levels were lower in C57L mice (24), this suggests that C57L mice might exhibit higher Ch absorption from both dietary and biliary sources compared with AKR mice. A putative Ch-transport protein (72) is believed to be located in the small intestinal brush-border membrane which might facilitate Ch absorption. It is possible that *Lith* genes may regulate the activity of Ch-transport proteins responsible for Ch absorption, or that the activity of a putative intestinal Ch-transport protein may be encoded or modified by one of the *Lith* genes.

A third function for *Lith* genes might be the encoding of proteins that affect mucin levels, as during lithogenesis there is a notable difference in mucin gel accumulation between C57L and AKR mice (Fig. 2). As inferred from our earlier prairie dog studies (44, 45), hypersynthesis and secretion of mucin glycoproteins are canonical responses to the lithogenity of gallbladder bile. The *Muc1* and *3* genes that regulate mucin secretion in the mouse gallbladder are located on mouse chromosomes 3 and 5 (73, 74), respectively, and therefore are not candidates for structural *Lith* genes (24). Hypersecretion of mucin and its gelation in gallbladders of C57L and F_1 mice also suggests that one of the *Lith* gene products might indirectly regulate mucin synthesis and secretion. Alteratively, the *Muc* gene expression may respond to a molecular stimulus from the lumen such as from higher content of Ch, Ca^{2+}, TCDC, TDC, or ATP (52) in gallbladder bile.

The remaining function for *Lith* genes would be the protein molecules responsible for the dramatic differences in the gallbladder sizes both prior to and after feeding the lithogenic diet. Because the CCK-A receptor (75) and *Cck* genes (76) map to mouse chromosomes 5 and 9, respectively, they are not candidate *Lith* genes (24). Nevertheless, the larger gallbladders displayed by C57L and F_1 mice suggest that *Lith* genes might inhibit gene expression, leading to defects in gallbladder motility. In addition, mucosal absorption of higher Ch contents in the gallbladder could impair gallbladder smooth muscle contraction, as accumulating evidence suggests (77).

The physical-chemical phenotypes of *Lith* genes in gallbladder bile described in the present study will be crucial for elucidating the genetic determinants of Ch gallstone disease in mice as well as in humans. This study therefore provides the connection between multiple *Lith* genes and early Ch gallstone disease and constitutes the basic framework for investigating how individual *Lith* genes influence the various Ch gallstone phenotypes. As there is exceptionally close homology between mouse and human genomes, this work should also facilitate a more rational search for human Ch gallstone (*LITH*) genes.

We are greatly indebted to Mark Hunt (The Jackson Laboratory) and Monika R. Leonard (Brigham and Women's Hospital) for excellent technical assistance. We also thank Dr. Kenneth D. R. Setchell, Department of Pediatrics at Children's Hospital Medical Center, Cincinnati, Ohio, for mass spectrometric analyses of mouse biles that proved that tauro-ω-muricholate was the lesser muricholate in C57L and AKR strains and that delta 22 bile salts were not a component as they are in the rat. We also thank Drs. Frank Lammert and David E. Cohen for their scientific advice and encouragement. Dr. Wang is a recipient of an Industry Research Scholar Award from American Digestive Health Foundation/American Gastroenterological Association (1996–99). This work was supported in part by research and center grants DK 34584 (D. Q-H. W.), DK 51553 and HL 32087 (B. P.), DK 36588 and DK 34854 (M. C. C.) all from the National Institutes of Health (US Public Health Service).

Manuscript received 21 January 1997 and in revised form 20 March 1997.

REFERENCES

1. Afdhal, N. H., and M. C. Carey. 1995. New perspectives on gallstone pathogenesis and prevention. *J. Ir. Coll. Phys. Surg.* **24:** 267–278.
2. Apstein, M. D., and M. C. Carey. 1996. Pathogenesis of cholesterol gallstones: a parsimonious hypothesis. *Eur. J. Clin. Invest.* **32:** 343–352.
3. Sampliner, R. E., P. H. Bennett, L. J. Comess, F. A. Rose, and T. A. Burch. 1970. Gallbladder disease in Pima Indians. Demonstration of high prevalence and early onset by cholecystography. *N. Engl. J. Med.* **283:** 1358–1364.
4. Thistle, J. L., and L. J. Schoenfield. 1971. Lithogenic bile among young Indian women. Lithogenic potential decreased with chenodeoxycholic acid. *N. Engl. J. Med.* **284:** 177–181.
5. Weiss, K. M., R. E. Ferrell, C. L. Hanis, and P. N. Styne. 1984. Genetics and epidemiology of gallbladder disease in New World Native peoples. *Am. J. Hum. Genet.* **36:** 1259–1278.
6. Covarrubias, C., V. Valdivieso, and F. Nervi. 1984. Epidemiology of gallstone disease in Chile. *In* Epidemiology and Prevention of Gallstone Disease. L. Capocaccia, G. Ricci, M. Angelico, and A. F. Attili, editors. Lancaster, MTP Press. 26–30.
7. Comess, L. J., P. H. Bennett, and T. A. Burch. 1967. Clinical gallbladder disease in Pima Indians: its high prevalence in contrast to Framingham, Massachusetts. *N. Engl. J. Med.* **277:** 894–898.
8. Sama, C., A. M. Morselli-Labate, F. Taroni, and L. Bar-

bara. 1990. Epidemiology and natural history of gallstone disease. *Semin. Liver Dis.* **10:** 149–158.
9. Jørgensen, T. 1988. Gallstones in a Danish population: familial occurrence and social factors. *J. Biosoc. Sci.* **20:** 111–120.
10. Jackson, C. E., and B. C. Gay. 1959. Inheritance of gallbladder disease. *Surgery.* **46:** 853–857.
11. Van der Linden, W. 1973. Genetic factors in gallstone disease. *Clin. Gastroenterol.* **2:** 603–614.
12. Van der Linden, W., and N. Simonsen. 1973. The familial occurrence of gallstone disease. Incidence in parents of young patients. *Hum. Hered.* **23:** 123–127.
13. Huddy, G. P. B. 1925. A study of the family histories of 300 patients suffering from chronic upper abdominal lesion. *Lancet.* **269:** 276–278.
14. Gilat, T., C. Feldman, Z. Halpern, M. Dan, and S. Bar-Meir. 1983. An increased familial frequency of gallstones. *Gastroenterology.* **84:** 242–246.
15. Sarin, S. K., V. S. Negi, R. Dewan, S. Sasan, and A. Saraya. 1995. High familiar prevalence of gallstones in the first-degree relatives of gallstone patients. *Hepatology.* **22:** 138–141.
16. Danzinger, R. G., H. Gordon, L. J. Schoenfield, and J. L. Thistle. 1972. Lithogenic bile in siblings of young women with cholelithiasis. *Mayo Clin. Proc.* **47:** 762–766.
17. Kesäniemi, Y. A., M. Koskenvuo, M. Vuoristo, and T. A. Miettinen. 1989. Biliary lipid composition in monozygotic and dizygotic pairs of twins. *Gut.* **30:** 1750–1756.
18. Paigen, K. 1995. A miracle enough: the power of mice. *Nature Med.* **1:** 215–220.
19. Alexander, M., and O. W. Portman. 1987. Different susceptibilities to the formation of cholesterol gallstones in mice. *Hepatology.* **7:** 257–265.
20. Paigen, B. 1995. Genetics of responsiveness to high-fat and high-cholesterol diets in the mouse. *Am. J. Clin. Nutr.* **62:** 458S–462S.
21. Tepperman, J., F. T. Caldwell, and H. M. Tepperman. 1964. Induction of gallstones in mice by feeding a cholesterol–cholic acid-containing diet. *Am. J. Physiol.* **206:** 628–634.
22. Fujihira, E., S. Kaneta, and T. Ohshima. 1978. Strain difference in mouse cholelithiasis and the effect of taurine on the gallstone formation in C57BL/C mice. *Biochem. Med.* **19:** 211–217.
23. Dueland, S., J. Drisko, L. Graf, D. Machleder, A. J. Lusis, and R. A. Davis. 1993. Effect of dietary cholesterol and taurocholate on cholesterol 7α-hydroxylase and hepatic LDL receptors in inbred mice. *J. Lipid Res.* **34:** 923–931.
24. Khanuja, B., Y-C. Cheah, M. Hunt, P. M. Nishina, D. Q-H. Wang, H. W. Chen, J. T. Billheimer, M. C. Carey, and B. Paigen. 1995. *Lith1,* a major gene affecting cholesterol gallstone formation among inbred strains of mice. *Proc. Natl. Acad. Sci. USA.* **92:** 7729–7733.
25. Wang, D. Q-H., and M. C. Carey. 1996. Complete mapping of crystallization pathways during cholesterol precipitation from model bile: influence of physical-chemical variables of pathophysiologic relevance and identification of a stable liquid crystalline state in cold, dilute, and hydrophilic bile salt-containing systems. *J. Lipid Res.* **37:** 606–630.
26. Cohen, D. E., and M. R. Leonard. 1995. Immobilized artificial membrane chromatography: a rapid and accurate HPLC method for predicting bile salt–membrane interactions. *J. Lipid Res.* **36:** 2251–2260.
27. Nishina, P. M., J. Verstuyft, and B. Paigen. 1990. Synthetic low and high fat diets for the study of atherosclerosis in the mouse. *J. Lipid Res.* **31:** 859–869.
28. Wang, D. Q-H., and M. C. Carey. 1996. Characterization of crystallization pathways during cholesterol precipitation from human gallbladder biles: identical pathways to corresponding model biles with three predominating sequences. *J. Lipid Res.* **37:** 2539–2549.
29. Konikoff, F. M., D. S. Chung, J. M. Donovan, D. M. Small, and M. C. Carey. 1992. Filamentous, helical and tubular microstructures during cholesterol crystallization from bile: evidence that biliary cholesterol does not nucleate classic monohydrate plates. *J. Clin. Invest.* **90:** 1155–1160.
30. Hotchkiss, R. D. 1948. A microchemical reaction resulting in the staining of polysaccharide structures in fixed tissue preparations. *Arch. Biochem.* **16:** 131–135.
31. Bartlett, G. R. 1959. Phosphorous assay in column chromatography. *J. Biol. Chem.* **234:** 466–468.
32. Fromm, H., P. Amin, H. Klein, and I. Kupke. 1980. Use of a simple enzymatic assay for cholesterol analysis in human bile. *J. Lipid Res.* **21:** 259–261.
33. Turley, S. D., and J. M. Dietschy. 1978. Re-evaluation of the 3α-hydroxysteroid dehydrogenase assay for total bile acids in bile. *J. Lipid Res.* **19:** 924–928.
34. Rossi, S. S., J. L. Converse, and A. F. Hofmann. 1987. High pressure liquid chromatographic analysis of conjugated bile acids in human bile: simultaneous resolution of sulfated and unsulfated lithocholyl amidates and the common conjugated bile acids. *J. Lipid Res.* **28:** 589–595.
35. Goh, E. H., S. M. Colles, and K. D. Otte. 1989. HPLC analysis of desmosterol, 7-dehydrocholesterol, and cholesterol. *Lipids.* **24:** 652–655.
36. Carey, M. C. 1978. Critical tables for calculating the cholesterol saturation of native bile. *J. Lipid Res.* **19:** 945–955.
37. Carey, M. C., and D. M. Small. 1978. The physical chemistry of cholesterol solubility in bile. Relationship to gallstone formation and dissolution in man. *J. Clin. Invest.* **61:** 998–1026.
38. Juniper, K., Jr., and E. N. Burson, Jr. 1957. Biliary tract studies. II. The significance of biliary crystals. *Gastroenterology.* **32:** 175–208.
39. Loomis, C. R., G. G. Shipley, and D. M. Small. 1979. The phase behavior of hydrated cholesterol. *J. Lipid Res.* **20:** 525–535.
40. Akiyoshi, T., K. Uchida, H. Takase, Y. Nomura, and N. Takeuchi. 1986. Cholesterol gallstones in alloxan-diabetic mice. *J. Lipid Res.* **27:** 915–924.
41. Caldwell, F. T., Jr., K. Levitsky, and B. Rosenberg. 1965. Dietary production and dissolution of cholesterol gallstones in the mouse. *Am. J. Physiol.* **209:** 473–478.
42. Bergman, F., A. H. Juul, and W. van der Linden. 1970. Development and regression of morphological and biochemical changes in hamsters and mice fed a cholesterol cholic acid containing diet. *Acta Pathol. Microbiol. Scand.* **78:** 179–191.
43. Holzbach, R. T., and C. Corbusier. 1978. Liquid crystals and cholesterol nucleation during equilibration in supersaturated bile analogs. *Biochim. Biophys. Acta.* **528:** 436–444.
44. Lee, S. P., J. T. LaMont, and M. C. Carey. 1981. Role of gallbladder mucin hypersecretion in the evolution of cholesterol gallstones: studies in the prairie dog. *J. Clin. Invest.* **67:** 1712–1723.
45. Holzbach, R. T., C. Corbusier, M. Marsh, and H. K. Naito. 1976. The process of cholesterol cholelithiasis induced by diet in the prairie dog: a physiochemical characterization. *J. Lab. Clin. Med.* **87:** 987–998.

46. Marks, J. W., G. G. Bonorris, G. Albers, and L. J. Schoenfield. 1992. The sequence of biliary events preceding the formation of gallstones in humans. *Gastroenterology.* **103:** 566–570.
47. Shiffman, M. L., H. J. Sugerman, J. M. Kellum, W. H. Brewer, and E. W. Moore. 1991. Gallstone formation after rapid weight loss: a prospective study in patients undergoing gastric bypass surgery for treatment of morbid obesity. *Am. J. Gastroenterol.* **86:** 1000–1005.
48. Broomfield, P. H., R. Chopra, R. C. Sheinbaum, G. G. Bonorris, A. Silverman, L. J. Schoenfield, and J. W. Marks. 1988. Effects of ursodeoxycholic acid and aspirin on the formation of lithogenic bile and gallstones during loss of weight. *N. Engl. J. Med.* **319:** 1567–1572.
49. Shiffman, M. L., R. D. Shamburek, C. C. Schwartz, H. J. Sugerman, J. M. Kellum, and E. W. Moore. 1993. Gallbladder mucin, arachidonic acid and bile lipids in patients who develop gallstones during weight reduction. *Gastroenterology.* **105:** 1200–1208.
50. Montet, J-C., M. Parquet, E. Sacquet, A-M. Montet, R. Infante, and J. Amic. 1987. β-Muricholic acid, potentiometric and cholesterol-dissolving properties. *Biochim. Biophys. Acta.* **918:** 1–10.
51. Gum, J. R., Jr. 1992. Mucin genes and the proteins they encode: structure, diversity, and regulation. *Am. J. Respir. Cell. Mol. Biol.* **7:** 557–564.
52. Dray-Charier, N., A. Paul, L. Combettes, M. Bouin, M. Mergey, P. Balladur, J. Capeau, and C. Housset. 1997. Regulation of mucin secretion in human gallbladder epithelial cells: predominant role of calcium and protein kinase C. *Gastroenterology.* **112:** 978–990.
53. Carey, M. C., and W. C. Duane. 1994. Enterohepatic circulation. *In* The Liver: Biology and Pathobiology. I. M. Arias, J. L. Boyer, N. Fausto, W. B. Jakoby, D. A. Schachter, and D. A. Shafritz, editors. New York, Raven Press, Ltd. 719–767.
54. Hussaini, S. M., S. P. Pereira, G. M. Murphy, and R. H. Dowling. 1995. Deoxycholic acid influences cholesterol solubilization and microcrystal nucleation time in gallbladder bile. *Hepatology.* **22:** 1735–1744.
55. Stolk, M. F. J., B. J. M. van de Heijning, K. J. van Erpecum, A. M. W. C. van den Broek, W. Renooij, and G. P. van Berge-Henegouwen. 1994. The effect of bile acid hydrophobicity on nucleation of several types of cholesterol crystals from model bile vesicles. *J. Hepatol.* **20:** 802–810.
56. van de Heijning, B. J. M., M. F. J. Stolk, K. J. van Erpecum, W. Renooij, and G. P. van Berge-Henegouwen. 1994. The effects of bile salt hydrophobicity on model bile vesicle morphology. *Biochim. Biophys. Acta.* **1212:** 203–210.
57. Kibe, A., M. A. Dudley, Z. Halpern, M. P. Lynn, A. C. Breuer, and R. T. Holzbach. 1985. Factors affecting cholesterol monohydrate crystal nucleation time in model systems of supersaturated bile. *J. Lipid Res.* **26:** 1102–1111.
58. Schmitz, F., D. Q-H. Wang, M. Blaeker, M. Nguyen, M. Chiu, M. Beinborn, M. C. Carey, and A. S. Kopin. 1996. CCK-A receptor-deficient mice have increased susceptibility to cholesterol gallstones. *Hepatology.* **24:** 246A.
59. Wang, D. Q-H., F. Lammert, B. Paigen, and M. C. Carey. 1997. *Lith* genes induce biliary cholesterol hypersecretion as a prelude to cholesterol gallstone formation in inbred mice. *Gastroenterology.* **112:** A1411.
60. Lammert, F., D. Q-H. Wang, B. Paigen, and M. C. Carey. 1997. *Lith* genes modify hepatic activities of the major lipid regulatory enzymes during cholesterol gallstone formation in inbred mice. *Gastroenterology.* **112:** A1312.
61. Sundaresan, S., T. L. Yang-Fang, and U. Francke. 1989. Genes for HMG-CoA reductase and serotonin 1a receptor are on mouse chromosome 13. *Somat. Cell Mol. Genet.* **15:** 465–469.
62. Welch, C. L., Y-R. Xia, I. Shechter, R. Farese, M. Mehrabian, S. Mehdizadeh, C. H. Warden, and A. J. Lusis. 1996. Genetic regulation of cholesterol homeostasis: chromosomal organization of candidate genes. *J. Lipid Res.* **37:** 1406–1421.
63. Cali, J. J., C. L. Hsieh, U. Francke, and D. W. Russell. 1991. Mutations in the bile acid biosynthetic enzyme sterol 27-hydroxylase underlie cerebrotendinous xanthomatosis. *J. Biol. Chem.* **266:** 7779–7783.
64. Brown, M. S., and J. L. Goldstein. 1986. A receptor-mediated pathway for cholesterol homeostasis. *Science.* **232:** 34–47.
65. Acton, S., A. Rigotti, K. T. Lanschulz, S. Xu, H. H. Hobbs, and M. Krieger. 1996. Identification of scavenger receptor SR-B1 as a high density lipoprotein receptor. *Science.* **271:** 518–520.
66. Cooper, A. D. 1992. Hepatic clearance of plasma chylomicron remnants. *Semin. Liver Dis.* **12:** 386–396.
67. Fuchs, M., F. Lammert, D. Q-H. Wang, B. Paigen, M. C. Carey, and D. E. Cohen. 1997. Sterol carrier protein 2 (*Scp2*) but not phosphatidylcholine transfer protein (*Pctp*) gene expression is enhanced during cholesterol gallstone formation in mice. *Gastroenterology.* **112:** A1267.
68. Frank, S. L., B. A. Taylor, and A. J. Lusis. 1989. Linkage of the mouse LDL receptor gene on chromosome 9. *Genomics.* **5:** 646–648.
69. Welch, C. L., Y. R. Xia, J. T. Billheimer, J. F. Strauss 3rd, and A. J. Lusis. 1996. Assignment of the mouse sterol carrier protein gene (*Scp2*) to chromosome 4. *Mamm. Genome.* **7:** 624–625.
70. Xia, Y-R., D. R. Bachinsky, J. A. Smith, R. T. McCluskey, C. H. Warden, and A. J. Lusis. 1993. Mapping of the glycoprotein 330 (*Gp330*) gene to mouse chromosome 2. *Genomics.* **17:** 780–781.
71. Reynier, M. O., J. C. Montet, A. Gerolami, C. Marteau, C. Crotte, A. M. Montet, and S. Mathieu. 1981. Comparative effects of cholic, chenodeoxycholic, and ursodeoxycholic acids on micellar solubilization and intestinal absorption of cholesterol. *J. Lipid Res.* **22:** 467–473.
72. Thurnhofer, H., and H. Hauser. 1990. Uptake of cholesterol by small intestinal brush border membrane is protein-mediated. *Biochemistry.* **29:** 2142–2148.
73. Kingsmore, S. F., A. P. Spicer, S. J. Gendler, and M. F. Seldin. 1995. Genetic mapping of the tumor-associated mucin 1 gene on mouse chromosome 3. *Mamm. Genome.* **6:** 378–379.
74. Shekels, L. L., C. Lyftogt, M. Kieliszewski, J. D. Filie, C. A. Kozak, and S. B. Ho. 1995. Mouse gastric mucin: cloning and chromosomal localization. *Biochem. J.* **311:** 775–785.
75. Samuelson, L. C., M. S. Isakoff, and K. A. Lacourse. 1995. Localization of the murine cholecystokinin A and B receptor genes. *Mamm. Genome.* **6:** 242–246.
76. Friedman, J. M., B. S. Schneider, D. E. Barton, and U. Francke. 1989. Level of expression and chromosome mapping of the mouse cholecystokinin gene: implications for murine models of genetic obesity. *Genomics.* **5:** 463–469.
77. Yu, P., Q. Chen, K. M. Harnett, J. Amaral, P. Biancani, and J. Behar. 1995. Direct G protein activation reverses impaired CCK signaling in human gallbladders with cholesterol stones. *Am. J. Physiol.* **269:** G659–G665.